Biochemistry and Biophysics Reports 38 (2024) 101660

Contents lists available at ScienceDirect

Biochemistry and Biophysics Reports

journal homepage: www.elsevier.com/locate/bbrep

Antiphotoaging effects of solvent fractions isolated from *Allomyrina dichotoma* larvae extract

Kyong Kim [a], Eun-Young Park [b], Dong-Jae Baek [b], Chang-Seok Lee [c], Yoon Sin Oh [a,*]

[a] Department of Food and Nutrition, Eulji University, Seongnam, South Korea
[b] College of Pharmacy and Natural Medicine Research Institute, Mokpo National University, Jeonnam, South Korea
[c] Department of Beauty and Cosmetic Science, Eulji University, Seongnam, South Korea

ARTICLE INFO

Keywords:
Allomyrina dichotoma larvae
Ultraviolet B
Photo-aging
Human dermal fibroblast
Collagen

ABSTRACT

Skin aging is affected by a variety of factors, including ultraviolet rays, oxidative stress, medications, smoking, and genetics. Among them, photo-aging accounts for about 80% of skin aging. The present study was evaluated to verify the potential of *Allomyrina dichotoma* larvae, which has recently been attracting attention as an edible insect, as an anti-aging substance. UVB irradiation at 100 mJ/cm^2 was sufficient to induce photo-aging of fibroblasts within 24 h, which was alleviated after treatment with 70% ethanol extract of *Allomyrina dichotoma* larvae extract (ADLE). To obtain an extract from ADLE, which has a relatively high content of polyphenol compounds containing physiological activity, fractional solvent extraction was carried out using organic solvents such as hexane, chloroform, ethyl acetate, and butanol. Additionally, ethyl acetate and butanol fractions contributed to the inhibition of UVB-induced ROS production, cell damage, and senescence of fibroblasts. It was also confirmed that the two fractions can regulate the expression of MMP-1 and AP-1. In particular, the ethyl acetate fraction showed an excellent effect in recovering collagen decomposed by UVB. Therefore, these results suggest that ADLE has potential as a natural insect-derived biomaterial to inhibit UVB-induced photo-aging.

1. Introduction

The skin serves as the primary, crucial barrier that protects against external environmental factors such as infectious pathogens, chemicals, and ultraviolet (UV) rays. Additionally, it plays a role in minimizing water loss from the body. Skin aging takes place as a result of cell membrane damage caused by oxidized lipids and the subsequent loss of normal skin cell function [1]. UV radiation, a significant contributor to external aging, triggers the production of harmful reactive oxygen species (ROS) in epidermal cells. ROS naturally occur in the body and serve a protective role against external invasions. However, excessive production of ROS can result in damage to lipids, proteins, nucleic acids, and other cellular components. This oxidative stress caused by UV-induced ROS can lead to various diseases, including inflammation, aging, cancer, and diabetes [2,3].

Changes in protein production and structure of the extracellular matrix, such as collagen and elastin, which comprise skin connective tissues, are a characteristic of skin aging. In vivo, free radicals stimulate the activity of collagenases such as matrix metalloproteinases (MMPs) and impede collagen formation. Furthermore, an imbalance in the antioxidant defense system accelerates skin aging, resulting in rough, strained, and wrinkled skin [4,5].

Edible insects have potential as future resources, and their interest and importance are increasing. The Korean rhinoceros beetle adults (*Allomyrina dichotoma*), commonly found in mountainous forests, are popular for ornamental purposes, and their larvae have traditionally been used as medicinal foods in Korea. The medicinal effects of *A. dichotoma* larvae (ADL) include anti-hepatic fibrosis, anti-tumor, anti-inflammatory, anti-obesity, and endoplasmic reticulum stress-related antineurotic effects [6]. However, its effects on anti-aging have not been observed. While the association between skin aging and antioxidant components, such as phytochemicals, is well known, research on the physiologically active components of insects is still lacking, particularly in relation to skin aging.

This study aimed to identify antioxidant components and their capabilities through solvent fractionation based on the polarity of ADL extract (ADLE). ADLE, being an insect with a different antioxidant system compared to plants, provides an intriguing subject for investigation. Additionally, the study aimed to compare the inhibitory effects of UVB-induced skin aging using the identified fractions.

* Corresponding author. Department of Food and Nutrition, Eulji University, South Korea.
E-mail address: ysoh@eulji.ac.kr (Y.S. Oh).

https://doi.org/10.1016/j.bbrep.2024.101660
Received 19 November 2023; Received in revised form 16 January 2024; Accepted 5 February 2024

2. Materials and methods

2.1. Preparation of ADLE solvent fractions

ADL were supplied from Yechun Bugs land (Yecheon-gun, Gyungsangbuk-do, Korea). Aqueous ethanolic extraction of the ADL (ADLE) was performed as previously described [7]. For extraction of ADLE solvent fractions, ADLE dissolved in water was sequentially fractionated with equal volumes of *n*-hexane (He), chloroform (Ch), ethyl acetate (EA), 1-butanol (Bu), and distilled water (DW) at room temperature. Five fractions were concentrated, dissolved in sterile dimethyl sulfoxide (DMSO) or distilled water depending on the experimental application.

2.2. Total phenolic content and antioxidant activity

Total phenolic content was measured using the Folin–Ciocalteu reagent (Sigma, St. Louis, MO, USA). A standard curve was also plotted using gallic acid. Results are expressed as milligrams per gram of fraction of gallic acid equivalent (GAE). Antioxidant activity was evaluated using the 2,2-diphenyl-1-picrylhydrazyl (DPPH) assay with a synthetic radical, 2,2-diphenyl-1-picrylhydrazyl, according to the method reported by Blois et al. [8]. Antioxidant ability of the sample was expressed as IC_{50} values by DPPH.

2.3. Cell culture, UVB-irradiation and cell viability

Human dermal fibroblast (HDF) cells were obtained from American Type Culture Collection (PCS201-010), grown in Dulbecco's modified Eagle's medium (DMEM) (Welgene, Daegu, Korea) supplemented with 10% fetal bovine serum (FBS) (Gibco, USA) and 1% penicillin-streptomycin (Welgene) at 37 °C in a humidified atmosphere containing 5% CO_2 as previously described [9]. The cells were seeded in appropriate numbers on different plates according to experimental conditions and cultured to reach 70–80% confluence after 24 h of incubation. The cells were washed twice with Dulbecco's phosphate-buffered saline (DPBS), and cells thinly soaked with DPBS were irradiated with 20, 50, 100, and 1000 mJ/cm^2 of UVB, respectively, for a minimum of 10 s and a maximum of 3 min at 25 °C.

UVB was performed using a Vilber-Lourmat device (Marne-la Vallee, France), the lid of the dish was opened during irradiation to minimize the absorption of UVB rays from the plastic material. Following UVB irradiation, the cells were replaced with growth medium containing the indicated concentrations of samples and incubated for an additional 24 h.

Cell viability was determined using the 3-(4,5-dimethylthiazol-2-yl)-2,5-diphenyltetrazolium bromide (MTT, Duchefa Biochemie BV, Haarlem, Netherlands) colorimetric assay. MTT of 0.5 mg/mL was added to each well and further cultured for 2 h. After careful removal of the supernatant, insoluble formazan crystals were dissolved in 2-propanol and measured at 540 nm (TECAN Group Ltd, Shanghai, China).

2.4. Intracellular ROS measurement

Intracellular ROS production was detected using an oxidative-sensitive 2′,7′-dichlorodihydrofluorescein diacetate (DCFH-DA; Molecular probe) fluorescent probe according to the methods described previously [10]. Briefly, the cells were seeded in 96-well black clear bottomed plates (Corning Inc., Corning, NY, USA) at 5.0×10^4 cells and incubated for 24 h. After UVB irradiation or sample treatment as described above, the cells were incubated with 10 μM H_2-DCFDA in the dark for 30 min. The cells were washed with DPBS, and the resulting fluorescent compound (2′,7′-dichlorofluorescein, DCF) was detected with a fluorescence microplate reader at 485 nm (excitation) and 535 nm (emission).

2.5. Senescence-associated β-galactosidase assay

The senescence-associated β-galactosidase (SA-β-gal) were measured using beta-galactosidase assay kit (Thermo scientific, USA) following the manufacturer's protocol. The cells were incubated overnight in 100 mm diameter dish with 2.5×10^6 cells, UVB irradiation or sample treatment were performed as described above. After washing with DPBS, the cells were stirred for 5 min at room temperature with 500 μL M-PER™ mammalian protein extraction reagent according to the protocol, then an equal amount of β-galactosidase assay reagent was added and reacted at 37 °C for 30 min. Then, 100 μL β-galactosidase assay stop solution was added to each well and measured at 405 nm.

2.6. Mitochondrial membrane potential assay

The loss of mitochondrial membrane potential (ΔΨ) has been known as s a hallmark of apoptosis [11]. Intracellular mitochondrial membrane potential levels were measured based on fluorescence (ex. 550 nm/em. 600 nm for red fluorescence and ex. 485 nm/em. 535 nm for green fluorescence) using JC-1 Mitochondrial membrane potential detection kit (Biotium, Hayward, CA, USA) according to the manufacturer's instructions. Under the same conditions as the ROS measurement, cells were incubated at 37 °C for 15 min with 1× JC-1 reagent working solution, and then twice washed with DPBS. The cells stained with JC-1 were detected fluorescence microplate reader. The results were analyzed as the ratio of red fluorescence divided by green fluorescence and expressed as fold of control.

2.7. Determination of MMP-1 secretions by ELISA

The cells were plated in 6-well plates at a concentration of 5.0×10^5 cells, cultured for 24 h, then irradiated with 100 mJ/cm^2 UVB and treated with 100 μg/mL of each sample. Following 24 h of incubation, the culture supernatant was centrifuged at 10,000×*g* for 3 min and the supernatant was collected. The quantitative measurement of MMP-1 production was performed using the Human MMP-1 (Sandwich ELISA) ELISA kit (cat. number ab215083, Abcam) according to the manufacturer's instruction.

2.8. Western blotting

Western blot was conducted as previously described [7]. All of the 1'st antibodies were purchased from cell signaling technology (USA). Briefly, proteins of containing 5–20 μg were separated by SDS-PAGE, transferred onto nitrocellulose blotting membranes (Amersharm, GE Healthcare Life science, Germany) and reacted with 1'st antibodies of AP-1, MMP-1, COL1A1, and α-tubulin at a ratio of 1: 1000, respectively. Protein bands were detected using an ELC kit (Millipore, USA). The bands were quantified by Quantity 1 version 4.6.7 software (Bio-Rad Laboratories).

2.9. Statistical analysis

Results were repeated at least three times and expressed as mean ± SD (standard deviation). Statistical analysis was performed using SPSS 20.0 software (IBM SPSS ver. 20.0.0 for Windows; IBM Co., Armonk, NY, USA). The significance of the experiment was verified by one-way analysis of variance (ANOVA), and in case of significance, a post-hoc test was performed by Duncan's multiple range test ($p < 0.05$). The relationships between antioxidant activity and phenolic content in solvent fractions of ADLE were determined by calculating Pearson's correlation coefficients.

3. Results

3.1. Total polyphenol content and DPPH radical scavenging activity of solvent fractions from ADLE

In this study, we employed sequential fractionation with different solvents (He, EA, Ch, B, and DW) to isolate various fractions from ADLE. The antioxidant effect of these fractions was evaluated by measuring the total polyphenol content and DPPH scavenging activity. As indicated in Table 1, the total polyphenol content (mg GAE/g) of the ADLE fractions varied with Bu demonstrating the highest content followed by EA, and finally the DW. Numerous studies have established a causal relationship between total phenol content and antioxidant activity [12]. Therefore, we also examined the DPPH radical scavenging activity of these fractions. By comparing the IC_{50} values (mg/mL, where lower values indicate better scavenging ability) for each solvent fraction, we found that the Bu fraction exhibited the highest antioxidant effect, followed by DW and EA. The correlation between total phenol content and DPPH radical scavenging activity was described by the equation $y = -2.795x + 38.124$, with a Pearson correlation coefficient of determination (r) of $= 0.993$ ($p < 0.01$) (Table 1).

3.2. Effect of UVB irradiation on photo-aging in HDF cells

We aimed to investigate the optimal dose of UVB irradiation by exposing HDF cells to various levels (20, 50, 100, and 1000 mJ/cm^2) of UVB. We examined aging-related parameters to assess the effects. The results showed that cells exposed to 20 mJ/cm^2 did not exhibit significant changes, but the viability was significantly reduced in cells treated with 50 mJ/cm^2 of UVB compared to the non-treated cells (Fig. 1A). Intracellular ROS generation was significantly increased in HDF cells exposed to 100 mJ/cm^2 of UVB, but the level did not show a dose-dependent increase (Fig. 1B). Additionally, the activity of beta-galactosidase, a widely used indicator of cellular aging, was observed to increase in a dose-dependent manner upon 50 mJ/cm^2 UVB irradiation (Fig. 1C). It was also examined the expression levels of MMP-1 and COL1A1 in cells treated with 50 mJ/cm^2 UVB irradiation. The results showed a dose-dependent increase in MMP-1 expression and a decrease in COL1A1 expression (Fig. 1D). In addition, we found that the expression of activator protein 1 (AP-1) was detected at 50 mJ/cm^2 UVB irradiation and showed higher expression at a concentration of 100 mJ/cm^2. This observation suggests that 100 mJ/cm^2 UVB irradiation is the optimal concentration for inducing photo-aging in HDF cells.

Table 1
Total polyphenol content and DPPH radical scavenging activity of ADLE solvent fractions.

Allomyrina dichotoma larvae *solvent fractions*	Total phenolic contents[A] (mg GAE/g of extract)	DPPH radical scavenging activity IC_{50}[B] (mg/mL)	Pearson's r[C] (p value)
70% ethanol (ADLE)	8.62 ± 0.09^{b}	8.46 ± 0.01^{cd}	0.933 ($p < 0.01$)
Hexane (He)	3.50 ± 0.21^{c}	35.32 ± 2.32^{a}	
Chloroform (Ch)	3.93 ± 0.67^{c}	27.53 ± 1.00^{b}	
Ethyl acetate (EA)	10.29 ± 0.37^{b}	9.37 ± 0.04^{c}	
1-Butanol (Bu)	14.62 ± 0.02^{a}	3.80 ± 0.23^{e}	
Water (DW)	8.96 ± 0.24^{b}	6.55 ± 0.03^{d}	

[a] Expressed as mg of gallic acid equiv/g of dry weight of residue.
[b] Concentration of extract residue required to inhibit 50% of the control calculated from linear regression equation in semilogarithmic manner.
[c] Pearson's correlation analysis between total phenolic content and antioxidant activity of solvent fractions of ADLE measured by DPPH method.

3.3. Effect of ADLE solvent fractions on ROS generation, mitochondrial dysfunction, and SA-β-galactosidase activity in UVB-induced HDF cells

To assess the cytotoxicity of the ADLE solvent fractions, HDF cells were treated with various concentrations (50–1000 μg/mL) of the ADLE solvents for 24 h, and cell viability was evaluated using the MTT assay. Fig. 2A shows that the polar solvent fractions (EA and Bu) were found to be non-toxic within the concentration range of up to 1000 μg/mL. However, the nonpolar solvent fraction, such as hexane and chloroform, exhibited toxicity at concentrations above 200 μg/mL. Consequently, a non-cytotoxic dose of 100 μg/mL for each of the five solvent fractions was selected for treatment in UVB-induced HDF cells. UVB irradiation at 100 mJ/cm^2 resulted in a decrease of approximately 24% ($p < 0.001$) in HDF cell viability, as depicted in Fig. 2B. No proliferative effect of the extracts was observed.

ROS generation was increased by 1.8-fold ($p < 0.001$) in UVB-treated cells compared to CON. However, treatment with polar solvent fractions EA ($p < 0.001$, Bu ($p < 0.001$), and DW ($p < 0.05$) significantly reduced intracellular ROS levels compared to the UVB alone, showing a similar effect to the ADLE group (Fig. 2C). Moreover, the number of SA-β-gal-stained cells, an indicator of cellular senescence, was increased by UVB irradiation, but it was decreased in the EA ($p < 0.01$) and Bu ($p < 0.01$) treatment groups compared to the control group (Fig. 2D). To investigate the effect of ADLE solvent fractions on mitochondrial membrane potential irradiated with UVB, JC-1-stained cells were measured [13]. The red/green fluorescence intensity of HDF cells was significantly decreased by approximately 21% ($p < 0.001$) after UVB irradiation compared to CON. However, co-treatment with the EA ($p < 0.05$), Bu ($p < 0.05$), and DW ($p < 0.05$) fractions increased the fluorescence levels, showing similar effects to the ADLE-treated cells (Fig. 2E).

3.4. Effect of the ethyl acetate fraction of ADLE on COL1A1 and MMP-1 levels in UVB-induced HDF cells

To evaluate the antioxidant and anti-aging effects of solvent fractionations of ADLE, we investigated the expression levels of proteins associated with collagen synthesis in UVB-treated HDF cells. We observed that UVB irradiation at 100 mJ/cm^2 increased the expression level of MMP-1. However, co-treatment with EA ($p < 0.05$), Bu ($p < 0.05$), or DW ($p < 0.05$) significantly inhibited the expression of MMP-1 (Fig. 3A and B). We next investigated the effect of ADLE solvent fractions on UVB-induced MMP-1 release from cells using ELISA assay. UVB irradiation increased the release of extracellular MMP-1 by 3.7-fold ($p < 0.001$). However, it was confirmed that EA treatments significantly ($p < 0.01$) reduced UVB-induced extracellular MMP-1 release (Fig. 3C).

Additionally, the treatment with solvent fractions of CH ($p < 0.01$), EA ($p < 0.001$), Bu ($p < 0.001$), and DW ($p < 0.001$) significantly inhibited the expression of AP-1, which was elevated by UVB irradiation (Fig. 3A and D). As shown in Fig. 3A and E, treatment with UVB significantly reduced the expression level of COL1A1 in HDF ($p < 0.001$). However, co-treatment with the EA fraction notably enhanced the expression level of COL1A1 ($p < 0.001$).

4. Discussion

Previously, we found that ADLE reduced ROS levels in both lipotoxicity-induced beta-cells [14] and LPS-treated Caco-2 cells [15], suggesting that ADLE has antioxidant effects. To elucidate the bioactive compounds of ADLE, it was extracted in hexane, chloroform, ethyl acetate, butanol, and water to obtain solvent fractions, and the total phenolic content and antioxidant activity of each fraction were measured and compared. The total polyphenol content of the ADLE fraction appeared in the order Bu > EA > DW > Ch > He, and the antioxidant activity increased in a dose-dependent manner. And the Pearson correlation coefficient between the two variables was 0.933, suggesting strong positive correlation.

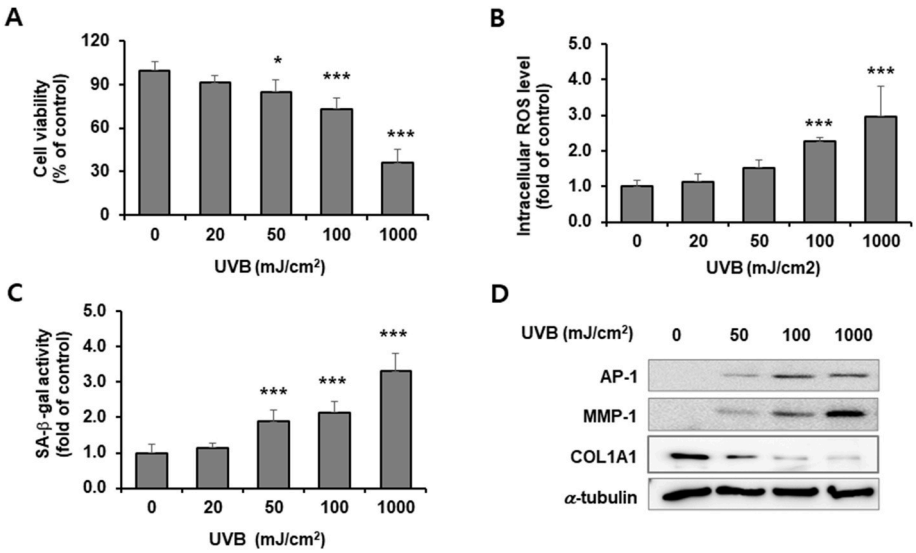

Fig. 1. Effect of UVB irradiation on photo-aging in HDF cells. HDF cells were irradiated with the indicated amount (20–1000 mJ/cm^2) of UVB and each activity was measured after 24 h incubation. (A) Cell viability was measured by MTT assay. (B) Intracellular ROS level was stained with DCFH-DA and analyzed by fluorescence reader. (C) Changes in SA-β-galactosidase activity was examined by commercial assay kit. (D) The protein expression levels of AP-1, MMP-1 and COL1A1 were measured according to the Western blot procedure. The results are shown as the means ± SD (n = 3–5), normalized to the percentage of non-irradiated control. *$p <$ 0.05 and ***$p < 0.001$ as compared to non-irradiated control.

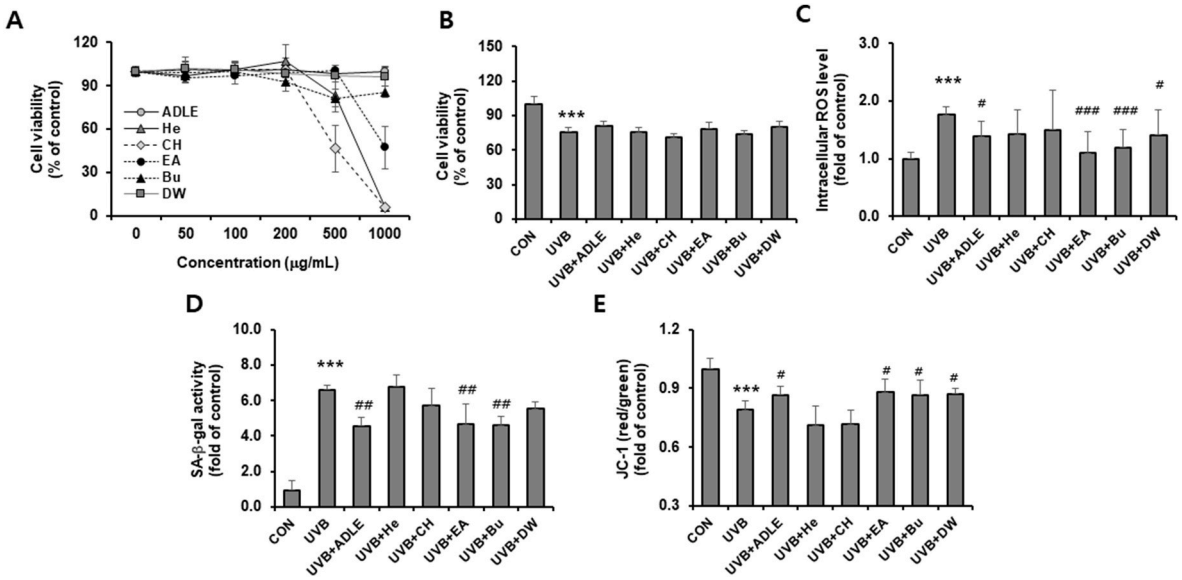

Fig. 2. Effect of ADLE solvent fractions on ROS generation, mitochondrial dysfunction, and SA-galactosidase activity induced by UVB in HDF cells. (A) Cells were treated with ADLE or its solvent fraction at various concentration for 24 h, and viability was measured by MTT. After 100 mJ/cm^2 UVB irradiation, cells were treated with ADLE or its solvent fractions at 100 μg/mL for 24 h and (B) cell viability was measured using MTT. (C) Intracellular ROS level was measured by DCFH-DA and (D) SA-β-galactosidase activity was examined by commercial assay kit. (E) Mitochondrial membrane potential was assayed by JC-1 detection kit. Data represent mean ± SD (n = 3–5), normalized to the percentage of CON. ***$p < 0.001$ versus CON. $^{\#}p < 0.05$, $^{\#\#}p < 0.01$, and $^{\#\#\#}p < 0.001$ versus UVB. CON: non-irradiated, UVB: 100 mJ/cm^2 UVB irradiated only.

Phenolic compounds are widely acknowledged for their diverse physiologically activities such as antibacterial, antioxidant, anti-inflammatory, and anticancer properties. Consequently, studies have been conducted to explore the extraction of phenolic compounds from natural sources [16]. Recently, research is being actively conducted on not only plant-derived antioxidants but also marine-derived antioxidants such as astaxanthin [17] and fucoidan [18].

In addition, researchers have shown keen interest in the phenolic compounds present in the epidermis, wings, and intestinal tract of insects that coexist in similar environmental conditions as plants [19]. It has been reported that bioactive phenolic compounds found in insects can be produced by the secondary metabolite of plant-derived compounds due to the nature of insects that eat plants, and new phenolic compounds are also synthesized during the sclerotization of insects [20]. The potential bioactive properties of these insect phenolic compounds may provide more health advantages in the prevention and therapy of human diseases besides their well-known nutritional value. Therefore, the diversification of extraction methods to isolate abundant phenolic compounds from insects is an immensely meaningful process.

UV radiation has a general effect on skin aging related to ROS generation due to energy absorption [21], and when photoaging parameters were measured after UVB irradiation, fibroblasts were found a

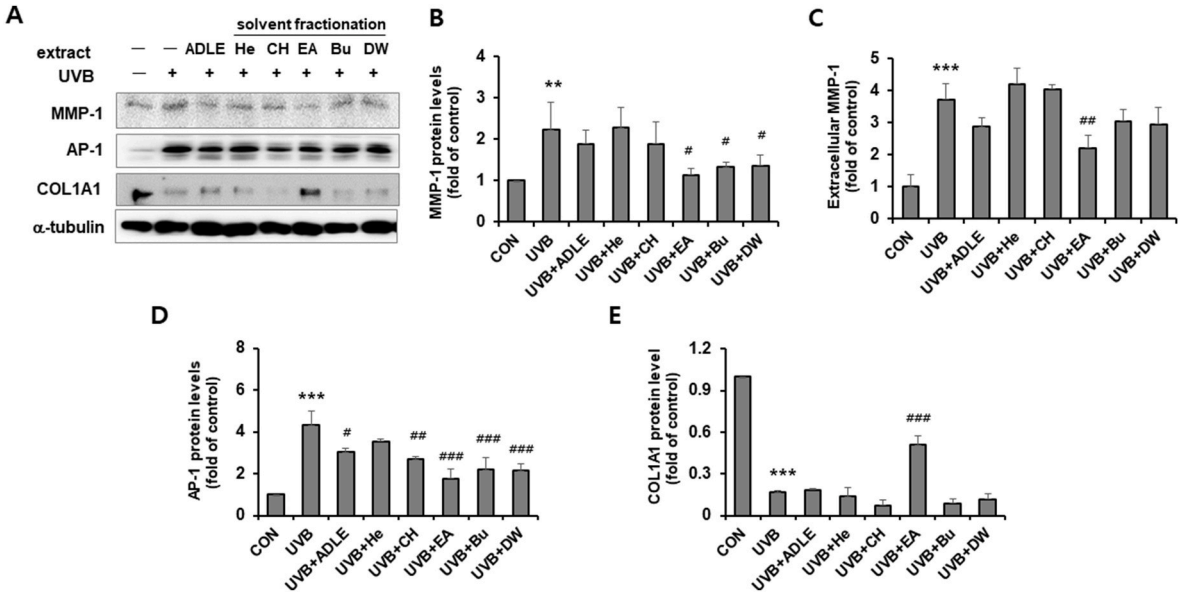

Fig. 3. Effect of ethyl acetate fraction of ADLE on UVB-induced COL1A1 and MMP-1 expression in HDF cells. After 100 mJ/cm^2 UVB irradiation, cells were treated with ADLE with or without its solvent fractions at 100 μg/mL for 24 h. (A) Protein expression levels of COL1A1, MMP-1 and AP-1 were measured according to the Western blot analysis and normalized to α-tubulin. (C) Extracellular MMP-1 production was measured using an ELISA kit. (B, D, E) The signal intensity was quantified using Image J software. CON: non-irradiated control, UVB: 100 mJ/cm^2 UVB-irradiated without sample. Values are presented as mean ± SD (n = 3–5), normalized to the percentage of CON. $^{**}p < 0.01$, $^{***}p < 0.001$ versus CON. $^{\#}p < 0.05$, $^{\#\#}p < 0.01$, and $^{\#\#\#}p < 0.001$ versus UVB. CON: non-irradiated, UVB: 100 mJ/cm^2 UVB irradiated only.

significant negative effects in relation to senescence. Above all, functional degeneration of mitochondria has been associated with aging-related features and is considered a major marker in many age-related diseases [22]. As a result of examining the effect of ADLE solvent fraction on the mitochondrial membrane potential irradiated with UVB, it could be confirmed that the membrane potential that decreased after UVB irradiation was recovered by treatment with EA and Bu.

Collagen accounts for approximately 80% of the human dermis, and type I collagen (COL1A1) is mainly found in extensible connective tissues, including the skin, respiratory and vascular systems [23]. Activation of AP-1, a critical regulator in the transcriptional control of matrix metalloproteinases (MMPs) responsible for collagen degradation, and subsequent decrease in COL1A1 expression are typical features of UVB-induced aging. These changes cause destruction of fibroblasts and collagen in wrinkles [24,25]. Hence, the identification of a substance that can promote procollagen synthesis by inhibiting the expression of MMPs and AP-1 holds great potential as a promising therapeutic strategy for addressing aging-related symptoms [26,27].

Through this study, it was confirmed that the ethyl acetate fraction of ADLE can contribute to a significant collagen recovery effect by suppressing the expression of MMP-1/AP-1. It is expected that this fraction is likely to contain more bioactive ingredients with antioxidant and anti-aging properties compared to other fractions.

This highlights its potential as a valuable preventive and therapeutic agent for combating photo-aging. Additional experiments are currently in progress to elucidate the precise protective mechanism of the EA fraction of ADLE against photo-aging. Furthermore, future clinical studies will involve the use of human *ex vivo* skin models.

Taken together, the ethyl acetate and butanol fractions of ADLE were shown to not only alleviate UVB-induced intracellular ROS production but also inhibit cell damage. The both fractions significantly contributed to suppress the expression of MMP-1 and AP-1, related collagenase enzyme, increased by UVB. It is judged to depend on the high polyphenol content and antioxidant capacity of the ethyl acetate and butanol fraction. What is noteworthy is that only the ethyl acetate fraction can significantly inhibit collagen degradation and participate in the prevention of photo-aging. These results suggest that ADLE's ethyl acetate fraction is valuable as a natural insect-derived biomaterial that can inhibit UVB-stimulated photo-aging.

CRediT authorship contribution statement

Kyong Kim: Writing – original draft, Validation, Investigation. **Eun-Young Park:** Methodology, Data curation. **Dong-Jae Baek:** Writing – review & editing, Resources. **Chang-Seok Lee:** Writing – original draft, Formal analysis, Data curation. **Yoon Sin Oh:** Writing – original draft, Funding acquisition, Conceptualization.

Declaration of competing interest

The authors declare no conflict of interest.

Acknowledgement

This study was supported by Basic Science Research Program Grant (NRF-2021R1F1A1050949) provided by the National Research Foundation of Korea (NRF), which is funded by the Ministry of Science, ICT and Future Planning.

Abbreviations

ADLE	*Allomyrina dichotoma* larvae extract
HDF	Human diploid fibroblast
UVB	ultraviolet B
ROS	Reactive oxygen species
MMPs	Matrix metalloproteinases
COL1A1	Collagen Type I alpha 1 chain

Appendix A. Supplementary data

Supplementary data to this article can be found online at https://doi.org/10.1016/j.bbrep.2024.101660.

References

[1] S. Silva, B. Michniak-Kohn, G.R. Leonardi, An overview about oxidation in clinical practice of skin aging, Anais brasileiros de dermatologia 92 (2017) 367–374, https://doi.org/10.1590/abd1806-4841.20175481.

[2] M. Valko, D. Leibfritz, J. Moncol, M.T.D. Cronin, M. Mazur, J. Telser, Free radicals and antioxidants in normal physiological functions and human disease, Int. J. Biochem. Cell Biol. 39 (2007) 44–84, https://doi.org/10.1016/j.biocel.2006.07.001.

[3] O.I. Aruoma, Free radicals, oxidative stress, and antioxidants in human health and disease, J. Am. Oil Chem. Soc. 75 (1998) 199–212, https://doi.org/10.1007/s11746-998-0032-9.

[4] J. Varani, D. Spearman, P. Perone, S.E. Fligiel, S.C. Datta, Z.Q. Wang, Y. Shao, S. Kang, G.J. Fisher, J.J. Voorhees, Inhibition of type I procollagen synthesis by damaged collagen in photoaged skin and by collagenase-degraded collagen in vitro, Am. J. Pathol. 158 (2001) 931–942, https://doi.org/10.1016/s0002-9440(10)64040-0.

[5] J.M. Catania, G. Chen, A.R. Parrish, Role of matrix metalloproteinases in renal pathophysiologies, Am. J. Physiol. Ren. Physiol. 292 (2007), https://doi.org/10.1152/ajprenal.00421.2006. F905-911.

[6] J. Kim, E.Y. Yun, S.W. Park, T.W. Goo, M. Seo, Allomyrina dichotoma larvae regulate food intake and body weight in high fat diet-induced obese mice through mTOR and mapk signaling pathways, Nutrients 8 (2016) 100, https://doi.org/10.3390/nu8020100.

[7] K. Kim, G. Bae, M. Lee, E. Park, D. Baek, C. Kim, H. Jun, Y. Oh, Allomyrina dichotoma Larva extract ameliorates the hepatic insulin resistance of high-fat diet-induced diabetic mice, Nutrients 11 (2019) 1522, https://doi.org/10.3390/nu11071522.

[8] M.S. Blois, Antioxidant determinations by the use of a stable free radical, Nature 181 (1958) 1199–1200, https://doi.org/10.1038/1811199a0.

[9] S.J. Ryu, K.A. Cho, Y.S. Oh, S.C. Park, Role of Src-specific phosphorylation site on focal adhesion kinase for senescence-associated apoptosis resistance, Apoptosis 11 (2006) 303–313, https://doi.org/10.1007/s10495-006-3978-9.

[10] A.R. Rosenkranz, S. Schmaldienst, K.M. Stuhlmeier, W. Chen, W. Knapp, G. J. Zlabinger, A microplate assay for the detection of oxidative products using 2',7'-dichlorofluorescin-diacetate, J. Immunol. Methods 156 (1992) 39–45, https://doi.org/10.1016/0022-1759(92)90008-h.

[11] J.D. Ly, D.R. Grubb, A. Lawen, The mitochondrial membrane potential (deltapsi (m)) in apoptosis; an update, Apoptosis 8 (2003) 115–128, https://doi.org/10.1023/a:1022945107762.

[12] G.K. Jayaprakasha, B.S. Patil, In vitro evaluation of the antioxidant activities in fruit extracts from citron and blood orange, Food Chem. 101 (2007) 410–418, https://doi.org/10.1016/j.foodchem.2005.12.038.

[13] M. Reers, T.W. Smith, L.B. Chen, J-aggregate formation of a carbocyanine as a quantitative fluorescent indicator of membrane potential, Biochemistry 30 (1991) 4480–4486, https://doi.org/10.1021/bi00232a015.

[14] K. Kim, M.-K. Kwak, G.-D. Bae, E.-Y. Park, D.-J. Baek, C.-Y. Kim, S.-E. Jang, H.-S. Jun, Y.S. Oh, Allomyrina dichotoma larva extract attenuates free fatty acid-induced lipotoxicity in pancreatic beta cells, Nutr. Res. Prac. 15 (2021) 294–308, https://doi.org/10.4162/nrp.2021.15.3.294.

[15] K. Kim, G.-D. Bae, E.-Y. Park, D.J. Baek, C.Y. Kim, S.-E. Jang, Y.S. Oh, Allomyrina dichotoma larval extract attenuates intestinal barrier disruption by altering inflammatory response and tight junction proteins in lipopolysaccharide-induced Caco-2 cells, Biochem. Biophys. Res. Commun. 532 (2020) 145–150, https://doi.org/10.1016/j.bbrc.2020.08.034.

[16] O.R. Alara, N.H. Abdurahman, C.I. Ukaegbu, Extraction of phenolic compounds: a review, Curr. Res. Food Sci. 4 (2021) 200–214, https://doi.org/10.1016/j.crfs.2021.03.011.

[17] R.R. Ambati, S.M. Phang, S. Ravi, R.G. Aswathanarayana, Astaxanthin: sources, extraction, stability, biological activities and its commercial applications–a review, Mar. Drugs 12 (2014) 128–152, https://doi.org/10.3390/md12010128.

[18] J.H. Lee, C.W. Yun, J. Hur, S.H. Lee, Fucoidan rescues p-cresol-induced cellular senescence in mesenchymal stem cells via FAK-akt-TWIST Axis, Mar. Drugs 16 (2018) 121, https://doi.org/10.3390/md16040121.

[19] F. Giampieri, J.M. Alvarez-Suarez, M. Machì, D. Cianciosi, M.D. Navarro-Hortal, M. Battino, Edible insects: a novel nutritious, functional, and safe food alternative, Food Frontiers 3 (2022) 358–365, https://doi.org/10.1002/fft2.167.

[20] M.C. Nino, L. Reddivari, C. Osorio, I. Kaplan, A.M. Liceaga, Insects as a source of phenolic compounds and potential health benefits, J. Insects Food and Feed 7 (2021) 1077–1087, https://doi.org/10.3920/jiff2020.0113.

[21] J.E. Sanches Silveira, D.M. Myaki Pedroso, UV light and skin aging, Rev. Environ. Health 29 (2014) 243–254, https://doi.org/10.1515/reveh-2014-0058.

[22] R. Bornstein, B. Gonzalez, S.C. Johnson, Mitochondrial pathways in human health and aging, Mitochondrion 54 (2020) 72–84, https://doi.org/10.1016/j.mito.2020.07.007.

[23] G.J. Fisher, S.C. Datta, H.S. Talwar, Z.-Q. Wang, J. Varani, S. Kang, J.J. Voorhees, Molecular basis of sun-induced premature skin ageing and retinoid antagonism, Nature 379 (1996) 335–339, https://doi.org/10.1038/379335a0.

[24] J. Kim, C.W. Lee, E.K. Kim, S.J. Lee, N.H. Park, H.S. Kim, H.K. Kim, K. Char, Y. P. Jang, J.W. Kim, Inhibition effect of Gynura procumbens extract on UV-B-induced matrix-metalloproteinase expression in human dermal fibroblasts, J. Ethnopharmacol. 137 (2011) 427–433, https://doi.org/10.1016/j.jep.2011.04.072.

[25] H.M. Chiang, H.C. Chen, H.H. Chiu, C.W. Chen, S.M. Wang, K.C. Wen, Neonauclea reticulata (havil.) merr stimulates skin regeneration after UVB exposure via ROS scavenging and modulation of the MAPK/MMPs/Collagen pathway, Evid Based Complement Alternat Med. (2013) (2013) 324864, https://doi.org/10.1155/2013/324864.

[26] E. Lam, R.T. Kilani, Y. Li, E.E. Tredget, A. Ghahary, Stratifin-induced matrix metalloproteinase-1 in fibroblast is mediated by c-fos and p38 mitogen-activated protein kinase activation, J. Invest. Dermatol. 125 (2005) 230–238, https://doi.org/10.1111/j.0022-202X.2005.23765.x.

[27] J. Lu, J.-H. Guo, X.-L. Tu, C. Zhang, M. Zhao, Q.-W. Zhang, F.-H. Gao, Tiron inhibits UVB-induced AP-1 binding sites transcriptional activation on MMP-1 and MMP-3 promoters by MAPK signaling pathway in human dermal fibroblasts, PLoS One 11 (2016) e0159998, https://doi.org/10.1371/journal.pone.0159998.